

# Design, fabrication, luminescence and biomedical applications of UCNPs@mSiO<sub>2</sub>-ZnPc-CDs-P(NIPAm-MAA) nanocomposite

Jiating Xu,<sup>a</sup> Dan Yang,<sup>a</sup> Ruichan Lv,<sup>a</sup> Bin Liu,<sup>a</sup> Shili Gai,<sup>a</sup> Fei He,<sup>a</sup> Chunxia Li,<sup>b</sup> and Piaoping Yang<sup>a\*</sup>

<sup>a</sup> Key Laboratory of Superlight Materials and Surface Technology, Ministry of Education, College of Material Sciences and Chemical Engineering, Harbin Engineering University, Harbin, 150001, P. R. China

<sup>b</sup> State Key Laboratory of Rare Earth Resource and Utilization, Changchun Institute of Applied Chemistry, Chinese Academy of Sciences, Changchun, 130022, P. R. China

\* Corresponding author: E-mail: [yangpiaoping@hrbeu.edu.cn](mailto:yangpiaoping@hrbeu.edu.cn) (P. Yang)

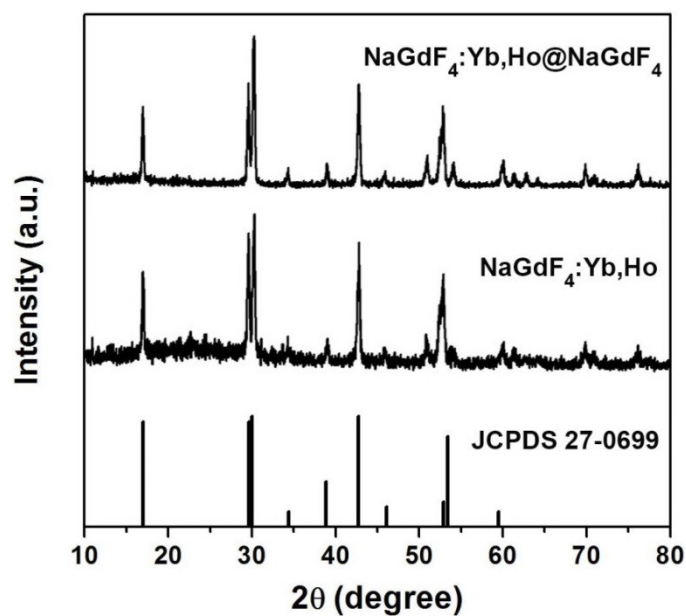


**Fig. S1** XRD patterns of NaGdF<sub>4</sub>:Yb,Ho core and NaGdF<sub>4</sub>:Yb,Ho@NaGdF<sub>4</sub> core-shell structured nanoparticles. The standard data lines of NaGdF<sub>4</sub> (JCPDS No.27-0699) are given for comparison.

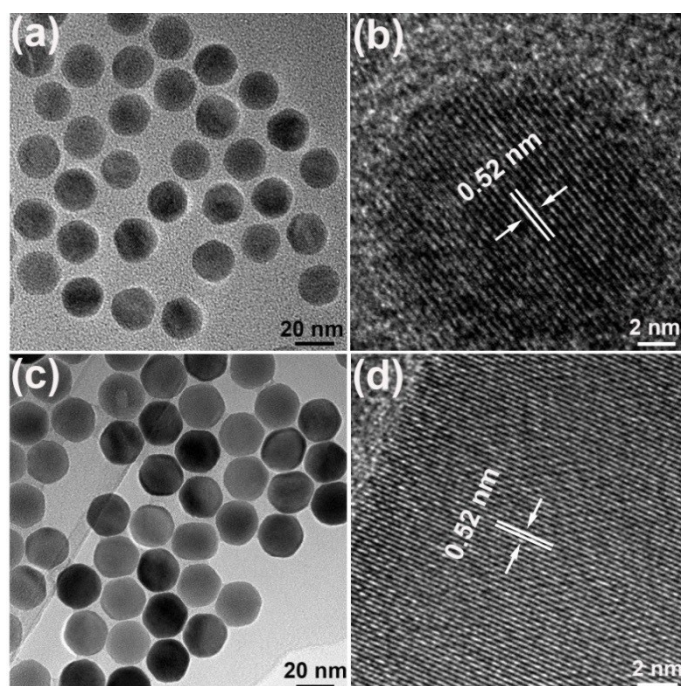


**Fig. S2** TEM and HRTEM image of NaGdF<sub>4</sub>:Yb,Ho (a, b) core and NaGdF<sub>4</sub>:Yb,Ho@NaGdF<sub>4</sub> (c, d) core-shell structured nanoparticles.

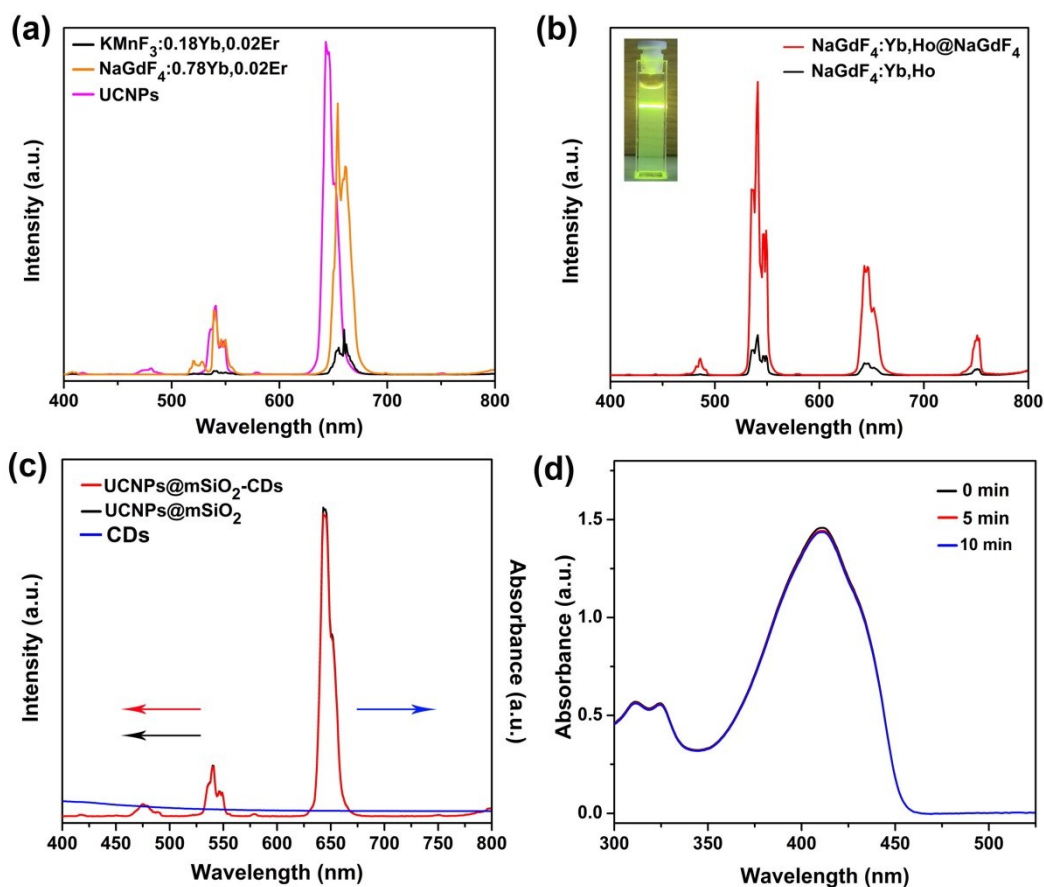


**Fig. S3** UC emission spectra of  $\text{KMnF}_3:\text{Yb,Er}$ ,  $\text{NaGdF}_4:\text{Yb,Er}$  and the UCNPs (a); UC emission spectra of  $\text{NaGdF}_4:\text{Yb,Ho}$  and  $\text{NaGdF}_4:\text{Yb,Ho}@ \text{NaGdF}_4$  core-shell nanoparticles (inset is the corresponding UCL images of core-shell nanoparticles); UC emission spectra of  $\text{UCNPs}@ \text{SiO}_2$  and  $\text{UCNPs}@ \text{SiO}_2\text{-CDs}$  and UV-vis absorption spectrum of CDs (c); UV-vis absorption spectra of DPBF solutions mixed with  $\text{UCNPs}@ \text{mSiO}_2\text{-CDs}$  under the irradiation of NIR laser with different times (d).

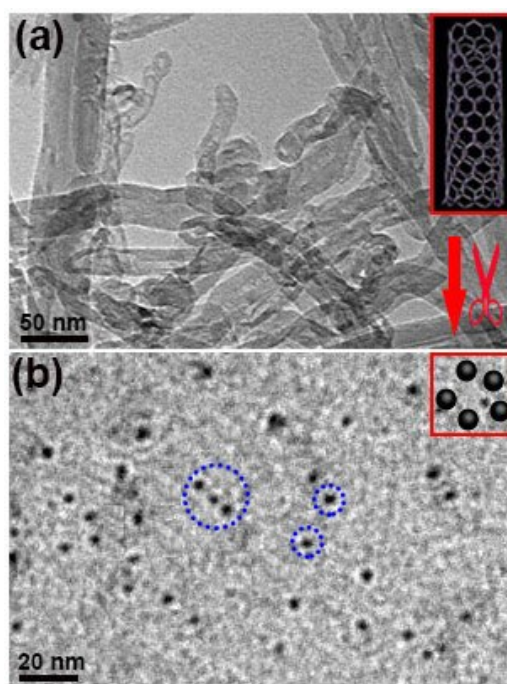


**Fig. S4** TEM images of carbon nanotubes (a) and carbon dots (b). Inset is the simulative structure of carbon nanotubes and carbon dots respectively.

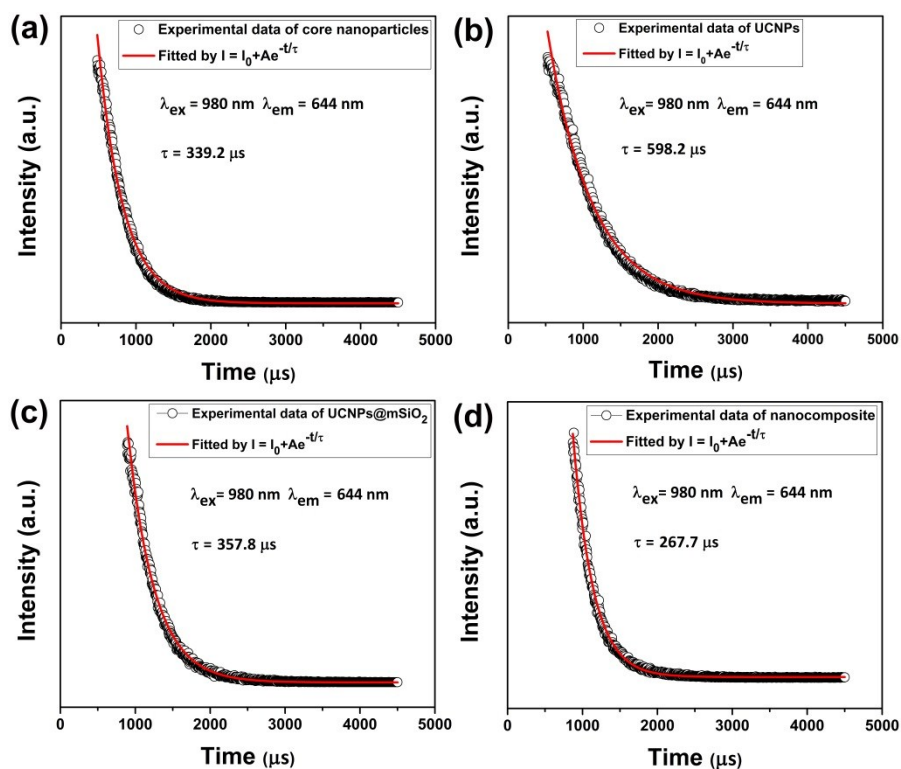


**Fig. S5** Decay curves of  $\text{Ho}^{3+}$  at 644 nm in core nanoparticles (A); core-shell structured UCNPs (B); UCNPs@mSiO<sub>2</sub> (C); UCNPs@mSiO<sub>2</sub>-ZnPc (D) under 980 nm NIR light excitation.

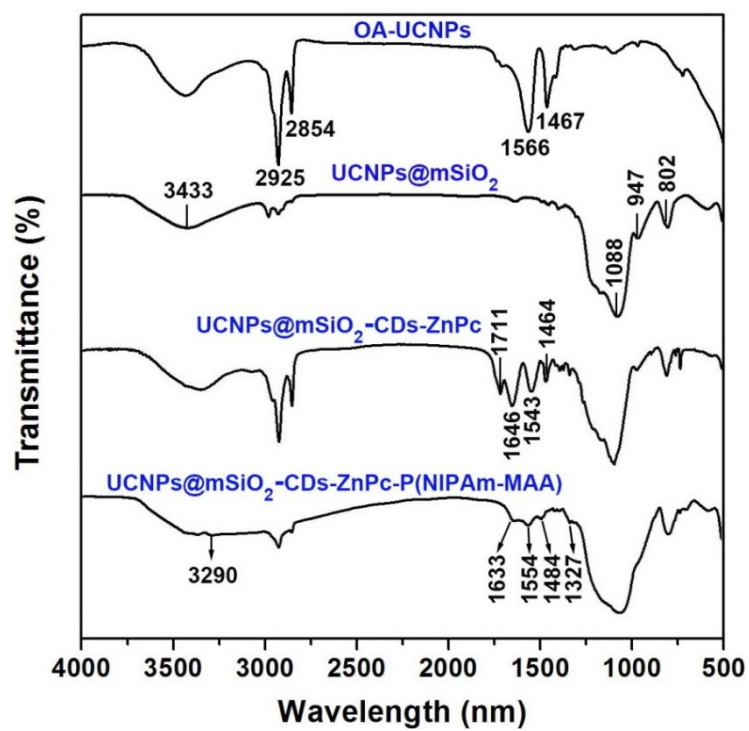


**Fig. S6** FT-IR spectra of OA-UCNPs, UCNPs@mSiO<sub>2</sub>, UCNPs@mSiO<sub>2</sub>-CDs-ZnPc, and UCNPs@mSiO<sub>2</sub>-CDs-ZnPc -P(NIPAm-MAA).

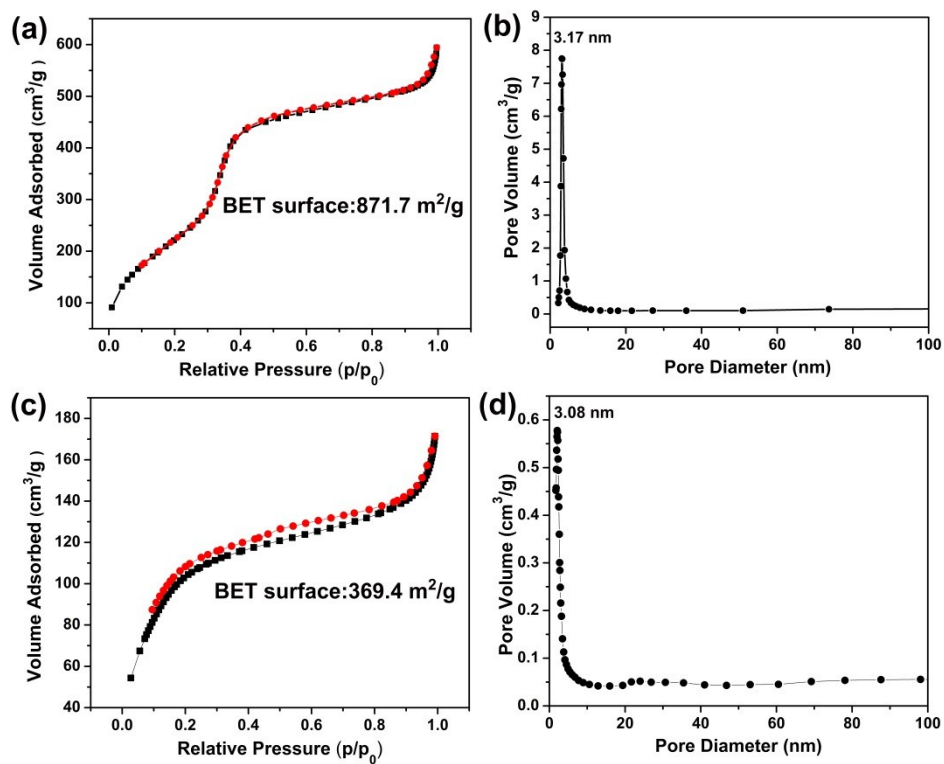


**Fig. S7**  $N_2$  adsorption/desorption isotherms and corresponding pore size distribution curves of UCNPs@mSiO<sub>2</sub> (a, b) and UCNPs@mSiO<sub>2</sub>-CDs-ZnPc spheres (c, d).

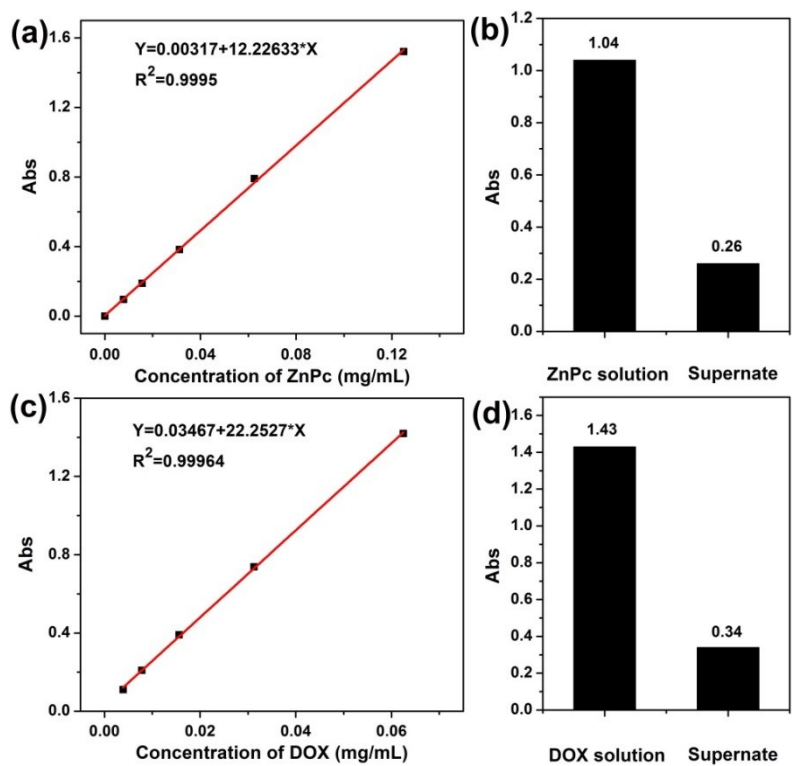


**Fig. S8** The standard curve for ZnPc (a) and DOX (c) detection at the absorbance wavelength of 665 nm and 480 nm respectively; the absorbance intensity for their initial solution and supernate before and after drug loading process (b, d)



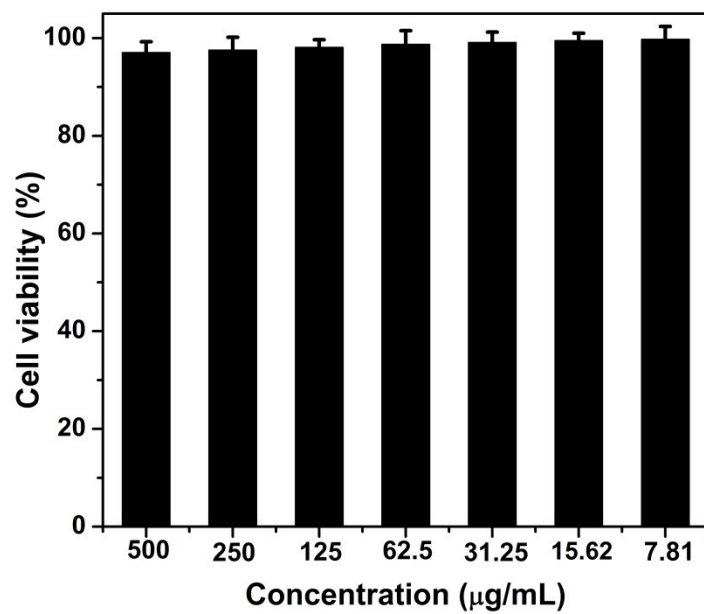


**Fig. S9** L929 fibroblast cell viability after incubating with UCNPs@mSiO<sub>2</sub>-P(NIPAm-MAA) nanocomposite for 24 h and quantitative assays by standard MTT method.

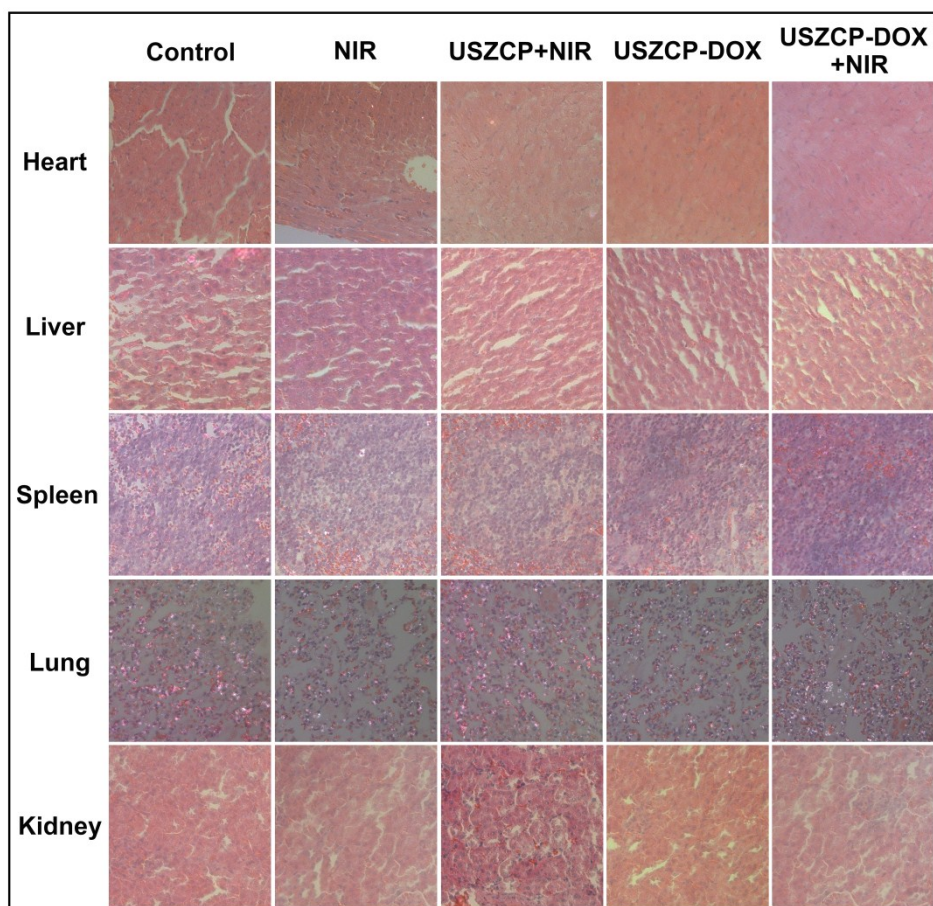


**Fig. S10** H&E stained images of heart, liver, spleen, lung, and kidney from different groups after 14 days treatment by USZCP nanocomposite.